Real-Time Contour Image Vectorization on GPU

Xiaoliang Xiong(✉), Jie Feng(✉), and Bingfeng Zhou

Institute of Computer Science and Technology, Peking University, Beijing, China
{jonny_xiong,feng_jie,cczbf}@pku.edu.cn

Abstract. In this paper, we present a novel algorithm to convert the contour in a raster image into its vector form. Different from the state-of-art methods, we explore the potential parallelism that exists in the problem and propose an algorithm suitable to be accelerated by the graphics hardware. In our algorithm, the vectorization task is decomposed into four steps: detecting the boundary pixels, pre-computing the connectivity relationship of detected pixels, organizing detected pixels into boundary loops and vectorizing each loop into line segments. The boundary detection and connectivity pre-computing are parallelized owing to the independence between scanlines. After a sequential boundary pixels organizing, all loops are vectorized concurrently. With a GPU implementation, the vectorization can be accomplished in real-time. Then, the image can be represented by the vectorized contour. This real-time vectorization algorithm can be used on images with multiple silhouettes and multi-view videos. We demonstrate the efficiency of our algorithm with several applications including cartoon and document vectorization.

Keywords: Vectorization · Real-time rendering · GPU acceleration

1 Introduction

Vector image is a compact form to represent image with a set of geometry primitives (like points, curves or polygons). It is independent with displaying resolution so that it can be rendered at any scale without aliasing. A raster image, in contrast, uses a large pixel matrix to store the image information, which requires much more space and conveys less semantics. It can be directly mapped onto display device and rendered with high efficiency, but suffers seriously from aliasing or loss of details when the image is scaled. The advantages of vector image over raster image, make it widely used in situations such as computer-aided design, on the Internet and plenty of practical applications.

Shape-from-Silhouette (SFS) is a specific application which adopts vector form as silhouette representation. It retrieves the 3D shape of the target object from multiple silhouette images taking at different viewpoints. In SFS, silhouette boundaries are approximated by line segments to simplify the computation and achieve the real-time rendering performance. Thus, an efficient algorithm to convert the silhouettes from pixels to vectors is essential. This is the motivation

© Springer International Publishing AG 2017
J. Braz et al. (Eds.): VISIGRAPP 2016, CCIS 693, pp. 35–50, 2017.
DOI: 10.1007/978-3-319-64870-5_2

of our work. Also, it is necessary to do the raster-to-vector conversion with high efficiency in applications like high-speed document scanning and cartoon animation.

Existing vectorization methods mainly focus on the accuracy during the conversion and ideally expect to approximate both the sharp and smooth features in the raster image with less geometry primitives. Triangular mesh [17], gradient mesh [12] and diffusion curves [10] are three commonly used geometry representatives. There are some researches adopt GPU to improve the rendering speed of constructed vector image [14], but the efficiency of the vector image construction is not high enough.

In contrast, we focus primarily on the silhouettes in the raster image and explore the potential parallelism in the problem to vectorize their contours as fast as possible. Both accuracy and efficiency are concerned to satisfy practical applications. Inspired by the scanline algorithm in polygon filling, we first detect the boundary pixels line by line in parallel, resulting in a set of unorganised pixels on each line. So secondly, the relationships of these pixels are computed. We note that only adjacent lines are directly related and each two lines can be processed simultaneously. Thirdly, all the boundary pixels are organized into loops based on pre-computed relationship. Fourthly, these loops which consist of boundary pixels can be vectorized into line segments concurrently. Hence, the problem is naturally decomposed into four steps and three steps can be parallelized. With this decomposition, our algorithm becomes not so sensitive to the image resolution.

Our key contribution is a novel algorithm that vectorizes the silhouettes in a raster image with high efficiency. We make a decomposition on the problem and take advantage of the potential parallelism to get an acceleration. We also apply the algorithm into several practical situations.

2 Related Work

Comparing to raster images, vector images has the advantages of more compact in presentation, requiring less space to store, convenient to transmit and edit, artifact-free in display etc. Image vectorization techniques aim at doing the raster-to-vector conversion accurately and efficiently. It includes crude vectorization on binary images and advanced vectorization on color images.

2.1 Image Vectorization

Crude Vectorization. Crude vectorization concerns grouping the pixels in the raster image into raw line fragments and representing the original image with primary geometry like skeleton and contour polygon. It is a fundamental process in the interpretation of image elements (like curves, lines) and can be used as preprocessing of applications like cartoon animation, topographic map reconstruction, SFS, etc.

Crude vectorization is often divided into two classes: *Thinning based methods* [11] and *Non-thinning based methods* [3]. The former first thin the rastered

object into a one-pixel-wide skeleton with iterative erosion, then these pixels are tracked into chain and approximated with line segments. The latter first extract the contour of the image, compute the medial axis between the contour pixels and then do the line segment approximation. *Thinning based methods* lose line width information during erosion and is time consuming. These disadvantages are compensated by *non-thinning based methods* that may have gaps at junctions. And both of these methods are sequential and need a long process time. [2] present a new medial axis pixel tracking strategy, which can preserve the width information and avoid distortion at junctions.

Advanced Vectorization. Advanced vectorization approaches concentrate on accurate approximation for all features in the raster image and take accuracy as their first consideration. *Triangle mesh based methods* [17] first sample important points in the image, then decompose this image into a set of triangles and store the corresponding pixel color on the triangle vertices. Inside each triangle, the color of each pixel can be recalculated through interpolation. [14] converts the image plane into triangular patches with curved boundaries instead of simple triangles and make the color distribution inside each patch more smooth. *Diffusion curve based methods* [10] first detect the edges in the original image, based on which it is converted into diffusion curve representation. Then a Poisson Equation is solved to calculate the final image. After vectorization by these methods, image can be effectively compressed, features are maintained or enhanced in different extent.

2.2 Image Vectorization in Applications

Cartoon Animation. In automatic cartoon animation, the artists only need to draw the key frames and in-betweens are generated by shape matching and interpolation. However, these techniques cannot be directly used in raster images, but are more suitable for vector-based graphics. Thus, a vectorization process is required to convert a raster key frame into its vector form. [18] subdivide the cartoon character into non-overlapping triangles based on which skeleton is extracted. Then artifacts are removed at the junction points and intersection areas by optimizing the triangles. There are also researches [16] on converting raster cartoon film into its vector form because the vector version is more easy to store, transmit, edit, display and so on. They take temporal coherence into consideration to alleviate flicker between cartoon frames.

Shape-from-Silhouette. Shape-from-Silhouette (SFS) is a method of estimating 3D shape of an object from its silhouette images. One famous SFS technique is the *visual hull* [6,8]. VH is defined as the maximal shape that reproduces the silhouettes of a 3D object from any viewpoint. It can be computed by intersecting the visual cones created by the viewing rays emanating from the camera center and passing through the silhouette contours, which is originally a chain of pixels. Most existing works adopt line segments as an approximation of the

silhouette contour to reduce large amount of redundant computation. The conversion from silhouette contour to line segments is originally a vectorization problem and efficient algorithm is needed to decrease time consumption in VH pre-computing.

Complex hardware like multi-processors [8] and distributed system [7] are adopted to do this step to guarantee the VH computation in real-time. There are many GPU-based methods [5,13,15] to accelerate the visual hull computation, for the VH algorithm is highly parallel. Thus, it is natural to think if the preprocessing can be parallelized, too. This is the motivation of our work and draws our attention mainly on the parallelization of contour vectorization.

Document Image Processing. Document processing is a complex procedure which evolves converting the text on paper or electronic documents into features the computer can recognize. [1] present a thinning algorithm based on line sweep operation, resulting in a representation with skeletons and intersection sets, that provides extra features for subsequent character recognition. It is efficient in computation comparing to pixel-based thinning algorithm [11] which outputs skeletons only.

GPU-Acceleration in Image Vectorization. Existing GPU related work is on the vectorized image rendering. [9] introduce a novel representation for random-access rendering of antialiased vector graphics. It has the ability to map vector graphics onto arbitrary surfaces, or under arbitrary deformations. [14] develop a real-time GPU-accelerated parallel algorithm based on recursive patch subdivision for rasterizing their vectorized results. [10] also propose a GPU implementation for rendering their vectorized images described by diffusion curves.

3 Our Algorithm

Our goal is to convert the silhouettes in an input image from raster to vector form with high efficiency and accuracy. The input image is preprocessed and converted into silhouette images by thresholding or background subtraction in advance. Intuitively, the boundary pixels are detected by scanning each line in these images. Since all scanlines are independent, the detection can be done concurrently. The resulting pixels on each line are then organized into *loops* based on their *connectivity relationship* with previous line, which can be precomputed in parallel. Finally, all organized loops are vectorized into line segments independently. Figure 1 shows the process of vectorizing a cartoon color image with our method. In the following, we describe each step in detail. To clarify the description, we refer *boundary* as unordered pixels, *loop* as an ordered pixel list and *contour* as all loops of a silhouette.

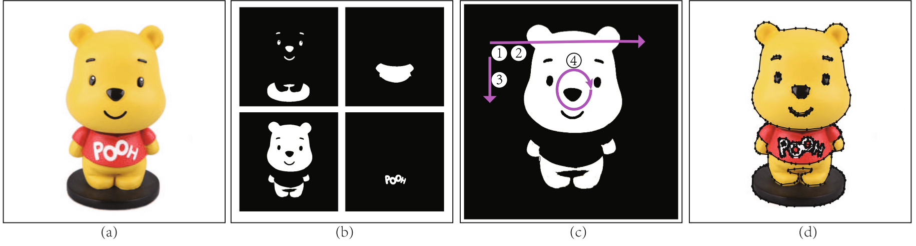

(a) (b) (c) (d)

Fig. 1. Vectorizing a cartoon color image with our method. (a) The input raster image. (b) The binary silhouettes. (c) The main procedure of our algorithm: ① parallel boundary detection and ② precontouring, ③ sequential contouring and ④ parallel contour vectorization. (d) The vectorization result. The contours are represented by line segments. The whole computation is completed in 9 ms, which provides possibility for real-time applications. (Color figure online)

3.1 Boundary Pixel Detecting

To rapidly extract the boundary pixels, we scan all lines in the silhouette images in parallel. A *scanline* $\hat{s}_i$ is a one-pixel-wide horizontal line that crosses the silhouette image from left to right. It is used to find the pairwise boundary pixels (I_k,O_k) of a foreground area. The collection of all scanlines are denoted as S,

$$S = \{\hat{s}_i | i = 1, \ldots, h\},$$

where h is the height of silhouette image. During scanning, when the scanline enters the foreground from background, the corresponding boundary pixel is recorded as I_k and when it leaves foreground into background, the boundary pixel is recorded as O_k. The point pair (I_k, O_k) is called an *interval* $R_k^{(i)}$ on $\hat{s}_i$, and the pixels between I_k and O_k belong to the foreground. All such pixel pairs on $\hat{s}_i$ consist its interval collection s_i,

$$s_i = \{R_k^{(i)} | R_k^{(i)} = (I_k, O_k), I_k < O_k, 1 \leq k \leq N_i\},$$

where line $\hat{s}_i$ has N_i intervals. Figure 2 shows an example of two scanlines $\hat{s}_{i_0}$ and $\hat{s}_{i_1}$. In each line, pixels are illustrated in different colors, where black indicates background, cyan for boundary pixels and gray for foreground. In the example, line $\hat{s}_{i_0}$ has 3 intervals and $\hat{s}_{i_1}$ has 4 intervals respectively.

As the independence of boundary pixel detection on each line $\hat{s}_i$, the scanning task of all lines S in the silhouette images can be allocated to multiple parallel threads, each for one scanline. This parallelization has an advantage: when the height of the image or the image number increases, we only need to add more threads and the running time is not affected too much. And it provides possibility for multiple images vectorization. The parallel scanning results in a group of foreground pixel intervals s_i on each line and the *connectivity relationship* between the lines should be computed in next step.

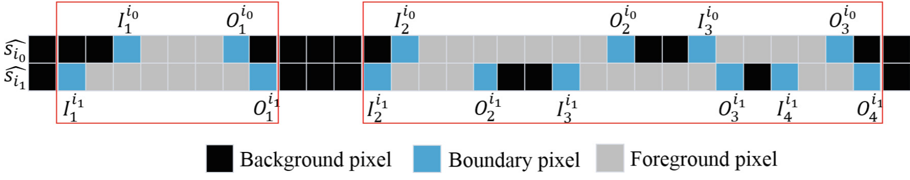

Fig. 2. Example of scanlines, intervals and segments. In this example, intervals on line $\hat{s}_{i_0}$ and $\hat{s}_{i_1}$ are divided into 2 segments, each marked with a red box. (Color figure online)

3.2 Pre-contouring

The detected boundary pixels are represented as foreground intervals s_i on each line $\hat{s}_i$. They should be organized into *loops* that enclose the object in the silhouette images. The target contour loops are denoted as B:

$$B = \{L_j | j = 1, \ldots, l\},$$

where l is the loop number and each loop L_j is a ordered list of boundary pixels:

$$L_j = \{p_m | m = 1, \ldots, M\},$$

That is, the loop L_j starts from p_1, goes along the silhouette and ends at p_M. If contour loops B are tracked directly on S, it is an up-down strategy that each loop stretches to pixels on next line if corresponding intervals are connected with current loop. The *connectivity relationship* between intervals on adjacent lines is needed during contour tracking and should be computed first.

For arbitrary two adjacent lines $\hat{s}_{i_0}$ and $\hat{s}_{i_1}$, their connectivity depends on the overlapping of their foreground intervals. If intervals $R_j^{(i_0)}$ in s_{i_0} and $R_k^{(i_1)}$ in s_{i_1} overlap, they consist a *segment*. In Fig. 2, $R_1^{(i_0)}$ and $R_1^{(i_1)}$ overlap, so they consist a segment, based on which we can infer these four boundary pixels are in the same loop. In this example, the rest of intervals on line $\hat{s}_{i_0}$ and $\hat{s}_{i_1}$ are divided into another segment and it has 3 intervals on i_1 and 2 on i_0 (3:2).

Theoretically, in the same segment the ratio of interval numbers on two adjacent lines can be classified into six cases:(1) *1:0* (2) *0:1* (3) *1:1* (4) *1:n* (5) *n:1* (6) *n:n* (Fig. 3). Case (1) and case (2) means interval only existing in one of the lines; Case (3) means that current loop does not change obviously from previous line to current line; case (4) and case (5) indicate loops merged or closed and new loops generated respectively; case (6) is a combination of case (4) and case (5). Each case indicates different change of loops in these lines and the boundary pixels of the included intervals are related.

Because this relationship computing depends only on the adjacent lines, it can be performed in parallel and separately accomplished as a pre-processing before contour organizing. Each parallel thread is responsible for dividing intervals on two lines into segments. With the connectivity relationship, we can organize each loop in order more efficiently.

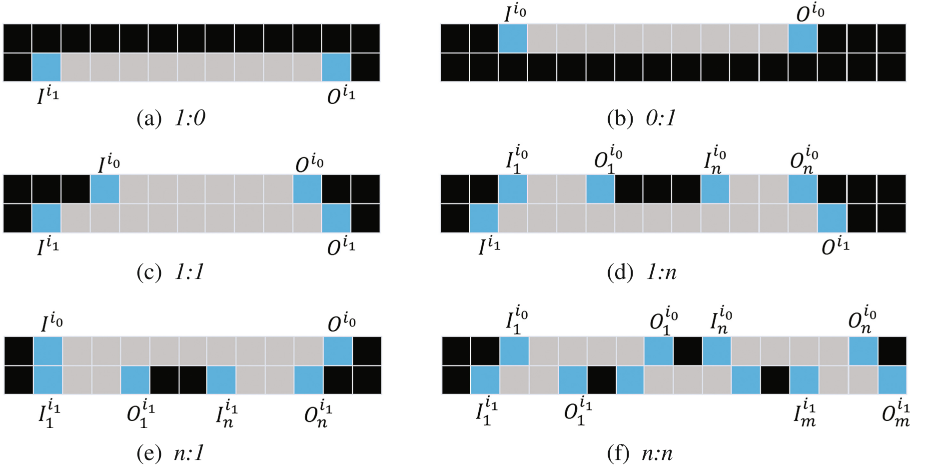

Fig. 3. Six cases of the connectivity relationship between intervals on two adjacent lines.

3.3 Contouring

Up to now, the boundary pixels are detected and pre-contoured in parallel, resulting in the foreground *intervals* and their *connectivity relationship* between adjacent lines. With these information, we can organize the boundary pixels into loops more easily, which is accomplished in each *segment*, according to the interval numbers in the two lines. During organizing, new loops may be generated, existing loops may be extended, merged, closed or branched from top to bottom in the image. The *connectivity relationship* between the two adjacent lines determines how the loop develops from the previous line to the current line, which can be directly represented by the interval numbers on each line $(|\{R_k^{(i_1)}\}| : |\{R_j^{(i_0)}\}|)$.

As described in Pre-contouring, in each individual segment, the *connectivity relationship* of adjacent lines can be classified into 6 cases, and each case means loop changes differently in these lines. Next, we will consider each case separately and show how the loops develop from previous line to current line as illustrated in Fig. 3.

– Loop Initialization (*1:0*)

During Contouring, a new loop is generated when new interval appears on current line, which does not overlap with any intervals on previous line. This loop records the boundary pixels of a presently separate region in the input image and will be complemented by the following pixels. As shown in Fig. 3(a), a loop starting from $I^{(i_1)}$ and ends at $O^{(i_1)}$ is generated.

– Loop Termination (*0:1*)

A loop is terminated when there is only an interval on the previous line in one segment. It indicates all pixels on a separate region are organised into a closed loop, which is called a *contour* in our algorithm. In Fig. 3(b), the corresponding loop of $I^{(i_0)}$ and $I^{(i_0)}$ is terminated.

- Loop Extension (*1:1*)

In one segment, if there is an interval on each line, it indicates the shape changes slightly in these two lines and the loop from the previous line can simply extend to the boundary pixels on current line. As shown in Fig. 3(c), for each interval in s_{i_0} and s_{i_1} :

$$s_{i_0} = \{R^{(i_0)} = (I^{(i_0)}, O^{(i_0)})\},$$
$$s_{i_1} = \{R^{(i_1)} = (I^{(i_1)}, O^{(i_1)})\},$$

we add boundary points $I^{(i_1)}$ and $O^{(i_1)}$ into the corresponding loops of $I^{(i_0)}$ and $O^{(i_0)}$, respectively.

- Loop Merging or Closing (*1:n*)

In this case, n intervals on the previous line change into one on current line. It means the loop number decreases and there are loops merged or closed. As shown in Fig. 3(d), there are n intervals in s_{i_0} and 1 interval in s_{i_1}:

$$s_{i_0} = \{R_j^{(i_0)} | R_j^{(i_0)} = (I_j^{(i_0)}, O_j^{(i_0)}), 1 \leq j \leq n\},$$
$$s_{i_1} = \{R^{(i_1)} = (I^{(i_1)}, O^{(i_1)})\}.$$

Hence, we add $I^{(i_1)}, O^{(i_1)}$ into the corresponding loops of $I_1^{(i_0)}, O_n^{(i_0)}$, respectively. For the rest of points in s_{i_0}, new pairs are formed as $(O_w^{(i_0)}, I_{w+1}^{(i_0)}), w = 0, \ldots,$ $n-1$. If the points of one pair belongs to the same loop, this loop will be closed, or else the different loops will be merged.

- Loop Branching (*n:1*)

On the contrary to the previous case, if 1 interval on previous line branches into n intervals on current line, new loops are generated to record the boundary pixels on the following line. In Fig. 3(e), there are n intervals in s_{i_1} and 1 interval in s_{i_0}:

$$s_{i_1} = \{R_k^{(i_1)} | R_k^{(i_1)} = (I_k^{(i_1)}, O_k^{(i_1)}), 1 \leq k \leq n\},$$
$$s_{i_0} = \{R^{(i_0)} = (I^{(i_0)}, O^{(i_0)})\}.$$

We add $I_1^{(i_1)}, O_n^{(i_1)}$ into the corresponding loop of $I^{(i_0)}, O^{(i_0)}$, respectively. For the left points in s_{i_1}, new pairs are formed as $(O_w^{(i_1)}, I_{w+1}^{(i_1)}), w = 0, \ldots, n-1$. Each pair is used for generating a new loop.

- Loop Merging(Closing) and Branching (*n:n*)

If there are more than 1 intervals on both lines in a segment, we can treat it as a combination of the case of loop merging(closing) and branching. In Fig. 3(f), there are n intervals in s_{i_0} and m intervals in s_{i_1}:

$$s_{i_0} = \{R_j^{(i_0)} | R_j^{(i_0)} = (I_j^{(i_0)}, O_j^{(i_0)}), 1 \leq j \leq n\},$$
$$s_{i_1} = \{R_k^{(i_1)} | R_k^{(i_1)} = (I_k^{(i_1)}, O_k^{(i_1)}), 1 \leq k \leq m\}.$$

We add $I_1^{(i_1)}, O_m^{(i_1)}$ into the corresponding loop of $I_1^{(i_0)}, O_n^{(i_0)}$, respectively. Loops are merged or closed for the rest of points in s_{i_0} and generated for the rest of points in s_{i_1}.

These six cases provide the rule for how to deal with boundary pixels on current line according to the *connectivity relationship* with previous line during loop organizing. This step must be in sequential manner because the boundary pixels on current line must be connected to the loops produced by previous boundary pixels. Furthermore, the computation need large memory to store the edge pixels and requires frequent memory access, which is the weakness of GPU. And this is the only step that has to be performed on CPUs. When all lines of silhouette images are processed, target loops B is generated.

3.4 Contour Vectorization

Using the method given above, the contour of the foreground can be described with a group of pixel loops B. Subsequently, we need to simplify each loop and approximate them with a set of line segments. Our approximation method is similar to the Active Contour Modeling [4]. Each loop $L_j = \{p_1 p_2 \cdots p_i \cdots p_{M-1} p_M\}$ is processed with a divide-and-conquer strategy. Let d be the maximum distance between the point p_i and line $p_1 p_M$:

$$d = max\{dist(p_i, \overrightarrow{p_1 p_M})\}.$$

if d is smaller than t (a constant threshold, we set t=1 in our experiment), $p_1 p_M$ is an approximate line segment and the discretization terminates. If not, loop L_j is divided into two sub-loops L_{j_0} and L_{j_1}:

$$L_{j_0} = \{p_1 p_2 p_i p_{\frac{M+1}{2}}\},$$
$$L_{j_1} = \{p_{\frac{M+1}{2}} \cdots p_j \cdots p_{M-1} p_M\}.$$

Then each sub-loop is tested iteratively until L_{j_0} or L_{j_1} satisfies the terminal condition or is small enough.

The vectorization of each loop is independent and we can process it with a GPU thread. When the loop number is small, the parallelism is limited and it has little improvement in performance comparing to processing each loop sequentially. The parallelizing of this step become more and more important as the increasing of the loop number.

When the four steps are completed, our algorithm can output a vector image with contour represented by line segments.

4 Experiment and Result

We implement our algorithm using CUDA on a common PC with Quad CPU 2.5 GHz, 2.75 GB RAM, and a GeForce GTX260+ graphic card. The vectorization task is decomposed into four steps, in which Boundary Detection and Pre-contouring are performed on GPU with multiple threads, each processing for different lines. Pre-contouring results are copied back to CPU for sequential computation of Contouring, and the organized contour loops are copied into the GPU for the final Vectorization.

Figures 4 and 5 show the vectorization results of some simple figures and characters. The former is used in silhouette-based applications(e.g. SFS) and the latter is inevitably used in document processing. The running time and the number of primitives used for vector representation are listed in Table 1.

4.1 Comparison

We compare our algorithm with a Floodfill-based method on time efficiency. The difference between them is the strategy of boundary pixel detection and ordering, and we use the same way to vectorize the contour loops. Floodfill based method iteratively searches the boundary pixels of the silhouette in neighborhood until all pixels are processed. Hence the running time increases exponentially with the image resolution and it depends heavily on the complexity of the scene. In contrast, our method detects and pre-contours the boundary pixels in parallel. The grouped pixels organizing depends a little on the image complexity, but not so sensitive thanks to the pre-contouring. Figure 6 shows the speed up ratio between Foodfill Based Method and our method on the three images with different resolution and gives the corresponding running time of each method. We can

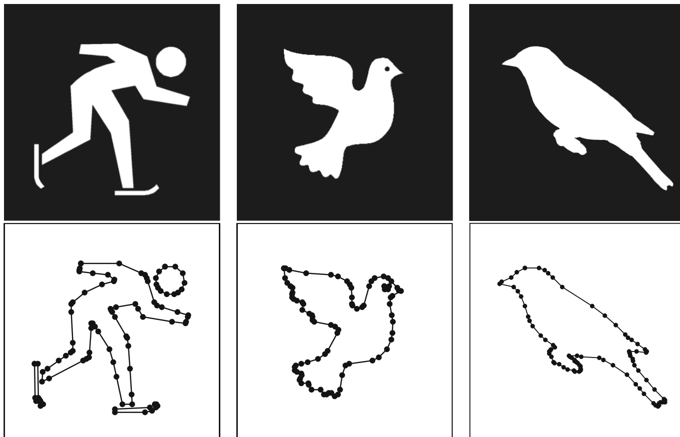

Fig. 4. Vectorization results of some figures. The first row shows the input raster images of some familiar figures(Skater, Pigeon, Bird.), and the second row lists corresponding vectorization results with contour represented by line segments.

Fig. 5. Vectorization results of different characters. The first, third and fifth rows are input raster images(English, Digit and Chinese characters respectively), the second, fourth and sixth rows are corresponding vectorization results with contour represented by line segments.

Table 1. Statistics of vectorization results and running time.

Image	Resolution	Points	Edges	Loops	Time(ms)
CharP	600 × 600	360	53	2	6.93
CharK	600 × 600	837	75	1	9.04
CharU	600 × 600	442	64	1	7.61
Digit4	600 × 600	414	24	2	5.93
Digit7	600 × 600	573	25	1	6.43
Digit8	600 × 600	1036	94	3	8.18
Chinese1	600 × 600	848	120	2	8.83
Chinese2	600 × 600	1080	223	7	10.73
Chinese3	600 × 600	1211	171	2	11.41
Pegion	400 × 400	439	86	2	5.89
Skater	400 × 400	596	104	4	6.56
Bird	600 × 480	833	83	1	8.92
Winnie	500 × 500	2761	432	26	8.54

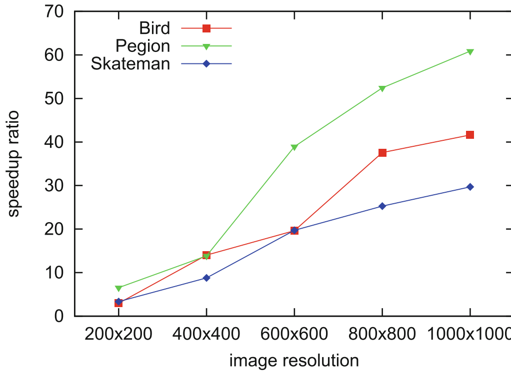

		200^2	400^2	600^2	800^2	1000^2
Pegion	FBM	29.91	105.39	306.41	510.11	799.78
	Ours	4.58	7.62	7.81	9.73	13.14
Skater	FBM	18.79	67.55	168.0	293.45	420.8
	Ours	5.62	7.73	8.52	11.61	14.17
Bird	FBM	14.51	90.53	158.26	419.94	583.28
	Ours	4.87	6.46	8.06	11.18	14.01

Fig. 6. Comparison between Floodfilled based method (FBM) and our method. The figure above shows the speedup ratio between two methods on different image resolution and the corresponding running time(ms) of each method is listed below.

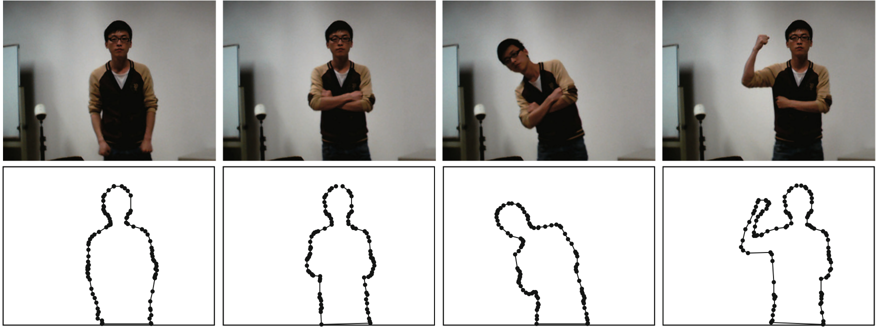

Fig. 7. Video vectorization. First row: four frames in the video. Second row: the corresponding vectorized results.

see that our method is not so sensitive to image resolution due to its parallelism and has a significant speed up especially under high image resolution.

4.2 Video Vectorization

Taking advantage of the fast speed, we apply our algorithm in video vectorization. Each frame is vectorized individually and we can achieve an average frame rate of 48 fps, which we believe will be even faster if the temporal coherence is considered. Figure 7 demonstrates the result.

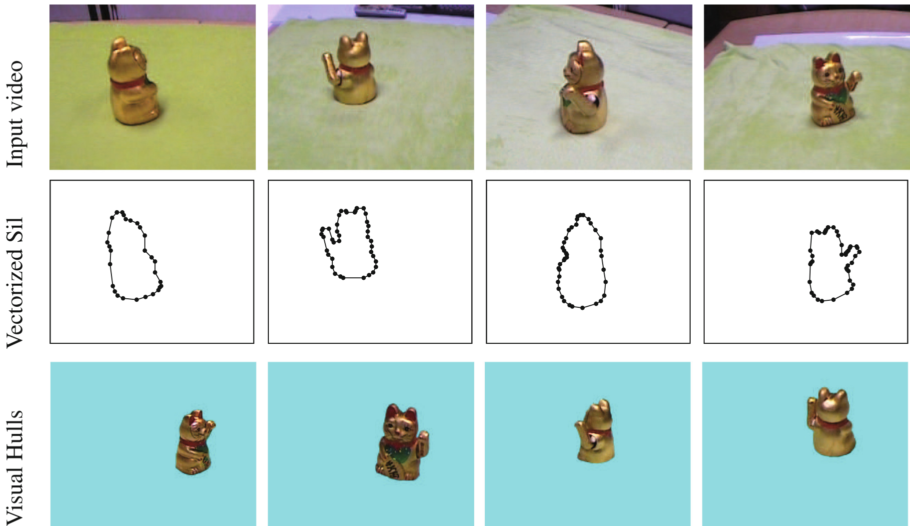

Fig. 8. Silhouettes vectorization in eight video streams and Visual Hull rendering based on the silhouettes. The first row shows 4 channel video images(eight in total), the second row is the corresponding vectorized silhouettes. Visual hulls are rendered from different viewpoints based on the silhouettes(the third row).

To further demonstrate the efficiency of our method, we perform the contour vectorization among 8-channel multi-view video streams simultaneously (which is a requirement of reconstructing dynamic visual hull) with image resolution of 600×480. Owing to the parallelization of our algorithm, the boundary pixels can be detected and pre-contoured in parallel among all video image lines at one time point. Then the pixels contouring can be parallelized between each video. Finally, each loop in the contour can be discretized into line segments in parallel. With the vectorization result, we can reconstruct and render dynamic VHs over 20 fps (Fig. 8).

4.3 Cartoon Image Vectorization

Figure 1 shows the vectorization of a cartoon image Winnie. We first binarize the input image according to the different colors and obtain a series of silhouettes. Then these silhouette images are vectorized simultaneously and result in a vector representation of the color image. Total computation can be accomplished in 9 ms.

Let life be beautiful like summer flowers

Rabindranath Tagore

Life, thin and light-off time and time again
Frivolous tireless

one
I heard the echo, from the valleys and the heart
Open to the lonely soul of sickle harvesting
Repeat outrightly, but also repeat the well-being of
Eventually swaying in the desert oasis

I believe I am
Born as the bright summer flowers
Do not withered undefeated fiery demon rule
Heart rate and breathing to bear the load of the cumbersome
Bored

Two
I heard the music, from the moon and carcass
Auxiliary extreme aestheticism bait to capture misty
Filling the intense life, but also filling the pure
There are always memories throughout the earth

I believe I am
Died as the quiet beauty of autumn leaves
Sheng is not chaos, smoke gesture
Even wilt also retained bone proudly Qing Feng muscle
Occult

Three
I hear love, I believe in love
Love is a pool of struggling blue-green algae
As desolate micro-burst of wind
Bleeding through my veins
Years stationed in the belief

I hear love, I believe in love

Fig. 9. Vectorization of a typed document page. Left: the input document, right: the vectorized result. The input image suffers from aliasing when the page is scaled and our result can keep the shape of each character well.

4.4 Document Image Vectorization

Document image vectorization is challenging for complex situations may appear in scanned document or handwritten pages and the number of contours may be large enough to bring difficulties in data storing and transferring on GPUs. To demonstrate the efficiency of our algorithm, we input a typed page at the resolution of 2500×1800, and the vectorization of the characters in this page can be done in 40 ms (Fig. 9). After vectorization, each character is represented with several line segments, which can be scaled without aliasing.

5 Conclusion

We propose a hardware-accelerated algorithm to vectorize the silhouettes in the raster image with high efficiency. The problem is decomposed into four steps and three of them can be parallelized significantly. We show the efficiency of our algorithm on some challenge applications including multiple videos and document image vectorization.

The limitation of our work lies in that the contouring step is still in sequential. One feasible way to alleviate the problem is to partition the silhouette image into several parts and the contouring among them can be parallelized. However, a merge step is needed if loops between two parts are connected, which will introduce extra computation cost. And we are exploring an ideal solution for this problem.

Acknowledgements. This work is partially supported by NSFC grants #61170206, #61370112, and Specialized Research Fund for the Doctoral Program of Higher Education #20110001110077.

References

1. Chang, F., Lu, Y.-C., Pavlidis, T.: Feature analysis using line sweep thinning algorithm. IEEE Trans. Pattern Anal. Mach. Intell. **21**(2), 145–158 (1999)
2. Dori, D., Liu, W.: Sparse pixel vectorization: an algorithm and its performance evaluation. IEEE Trans. Pattern Anal. Mach. Intell. **21**(3), 202–215 (1999)
3. Jimenez, J., Navalon, J.L.: Some experiments in image vectorization. IBM J. Res. Dev. **26**(6), 724–734 (1982)
4. Kass, M., Witkin, A., Terzopoulos, D.: Snakes: active contour models. Int. J. Comput. Vis. **1**(4), 321–331 (1988)
5. Ladikos, A., Benhimane, S., Navab, N.: Efficient visual hull computation for real-time 3d reconstruction using CUDA, pp. 1–8 (2008)
6. Laurentini, A.: The visual hull concept for silhouette-based image understanding. IEEE Trans. Pattern Anal. Mach. Intell. **16**(2), 150–162 (1994)
7. Li, M., Magnor, M., Seidel, H.-P.: A hybrid hardware-accelerated algorithm for high quality rendering of visual hulls. In: Proceedings of Graphics Interface 2004, pp. 41–48. Canadian Human-Computer Communications Society (2004)
8. Matusik, W., Buehler, C., Raskar, R., Gortler, S.J., McMillan, L.: Image-based visual hulls. In: SIGGRAPH 2000, pp. 369–374. ACM (2000)

9. Nehab, D., Hoppe, H.: Random-access rendering of general vector graphics. In: ACM Transactions on Graphics (TOG), vol. 27, p. 135. ACM(2008)
10. Orzan, A., Bousseau, A., Barla, P., Winnemöller, H., Thollot, J., Salesin, D.: Diffusion curves: a vector representation for smooth-shaded images. ACM Trans. Graph. **56**(7), 101–108 (2013)
11. Smith, R.W.: Computer processing of line images: a survey. Pattern Recogn. **20**(1), 7–15 (1987)
12. Sun, J., Liang, L., Wen, F., Shum, H.-Y.: Image vectorization using optimized gradient meshes. In: ACM Transactions on Graphics (TOG), vol. 26, p. 11. ACM (2007)
13. Waizenegger, W., Feldmann, I., Eisert, P., Kauff, P.: Parallel high resolution real-time visual hull on GPU. In: 2009 16th IEEE International Conference on Image Processing (ICIP), pp. 4301–4304 (2009)
14. Xia, T., Liao, B., Yu, Y.: Patch-based image vectorization with automatic curvilinear feature alignment. In: ACM Transactions on Graphics (TOG), vol. 28, p. 115. ACM (2009)
15. Yous, S., Laga, H., Kidode, M., Chihara, K.: GPU-based shape from silhouettes. In: Proceedings of the 5th International Conference on Computer Graphics and Interactive Techniques in Australia and Southeast Asia, pp. 71–77. ACM (2007)
16. Zhang, S.-H., Chen, T., Zhang, Y.-F., Hu, S.-M., Martin, R.R.: Vectorizing cartoon animations. IEEE Trans. Vis. Comput. Graph. **15**(4), 618–629 (2009)
17. Zhao, J., Feng, J., and Zhou, B.: Image vectorization using blue-noise sampling. In: IS&T/SPIE Electronic Imaging, p. 86640H. International Society for Optics and Photonics (2013)
18. Zou, J.J., Yan, H.: Cartoon image vectorization based on shape subdivision. In: Proceedings of the Computer Graphics International 2001, pp. 225–231. IEEE (2001)